J. Fluid Mech. (2014), *vol.* 741, R2, doi:10.1017/jfm.2014.1

JFM RAPIDS
journals.cambridge.org/rapids

Lagrangian cascade in three-dimensional homogeneous and isotropic turbulence

Yongxiang Huang[1,†] and François G. Schmitt[2,3,4]

[1]Shanghai Institute of Applied Mathematics and Mechanics, and Shanghai Key Laboratory of Mechanics in Energy Engineering, Shanghai University, Shanghai 200072, PR China

[2]Université Lille Nord de France, F-59000 Lille, France

[3]USTL, LOG, F-62930 Wimereux, France

[4]CNRS, UMR 8187, F-62930 Wimereux, France

(Received 21 October 2013; revised 21 December 2013; accepted 30 December 2013)

In this work, the scaling statistics of the dissipation along Lagrangian trajectories are investigated by using fluid tracer particles obtained from a high-resolution direct numerical simulation with $Re_\lambda = 400$. Both the energy dissipation rate ϵ and the local time-averaged ϵ_τ agree rather well with the lognormal distribution hypothesis. Several statistics are then examined. It is found that the autocorrelation function $\rho(\tau)$ of $\ln(\epsilon(t))$ and variance $\sigma^2(\tau)$ of $\ln(\epsilon_\tau(t))$ obey a log-law with scaling exponent $\beta' = \beta = 0.30$ compatible with the intermittency parameter $\mu = 0.30$. The qth-order moment of ϵ_τ has a clear power law on the inertial range $10 < \tau/\tau_\eta < 100$. The measured scaling exponent $K_L(q)$ agrees remarkably with $q - \zeta_L(2q)$ where $\zeta_L(2q)$ is the scaling exponent estimated using the Hilbert methodology. All of these results suggest that the dissipation along Lagrangian trajectories could be modelled by a multiplicative cascade.

Key words: homogeneous turbulence, intermittency, isotropic turbulence

1. Introduction

Turbulent flows are complex and multiscale and are characterized by eddy motions of different spatial sizes with different time scales (Frisch 1995; Pope 2000; Tsinober 2009). This has been described by Kolmogorov's scaling theory of turbulence in 1941. The scaling behaviour of the Eulerian velocity field has been studied in details to quantify the intermittent nature of turbulence for large Reynolds numbers and homogeneous turbulence (Frisch 1995; Sreenivasan & Antonia 1997). Here we consider the Lagrangian frame, in which the fluid particle is tracked experimentally

†Email address for correspondence: yongxianghuang@gmail.com

or numerically (Mordant *et al.* 2002; Yeung 2002; Chevillard *et al.* 2003; Biferale *et al.* 2004; Chevillard & Meneveau 2006; Xu *et al.* 2006*a*; Toschi & Bodenschatz 2009; Meneveau 2011). Fluid particles are fluctuating over different time scales with a power-law behaviour in the inertial range, e.g. $\tau_\eta \ll \tau \ll T_L$, in which τ_η is the Kolmogorov time scale, and T_L is the Lagrangian integral time scale. Conventionally, multiscale statistics are characterized by using the Lagrangian structure functions (LSFs), i.e. $S_L^q(\tau) = \langle |\Delta_\tau u(t)|^q \rangle \sim \epsilon^{q/2}\tau^{q/2}$ in which $\Delta_\tau u(t) = u(t+\tau) - u(t)$ is the Lagrangian velocity increment, and τ is the separation time scale and is lying in the inertial range. Recently, Huang *et al.* (2013) showed a clear Lagrangian inertial range on the frequency range $0.01 < \omega\tau_\eta < 0.1$ (respectively $10 < \tau/\tau_\eta < 100$) and retrieved the scaling exponent $\zeta_L(q)$ by using a Hilbert-based methodology. The measured scaling exponents $\zeta_L(q)$ are nonlinear and concave, showing that intermittency corrections are indeed relevant for Lagrangian turbulence (Borgas 1993; Chevillard *et al.* 2003; Biferale *et al.* 2004; Xu, Ouellette & Bodenschatz 2006*b*). Using a high-resolution Lagrangian turbulence database, we can now verify the scaling relations associated with the Kolmogorov refined similarity hypothesis (RSH).

2. Refined similarity hypothesis

Let us recall some main ingredients of the Lagrangian version of the Kolmogorov's refined similarity hypothesis (LRSH), in which the energy dissipation rate $\epsilon = 2\nu S_{ij}S_{ij}$ is involved. Here $S_{ij} = 1/2(\partial u_i/\partial x_j + \partial u_j/\partial x_i)$ is the velocity strain rate tensor along a Lagrangian trajectory. A local time average of the energy dissipation rate along a Lagrangian trajectory is defined as

$$\epsilon_\tau(t) = \frac{1}{\tau}\int_{0\leqslant t'\leqslant\tau} \epsilon(t+t')\,\mathrm{d}t', \quad X_\tau(t) = \ln(\epsilon_\tau(t)) \tag{2.1}$$

where $X_\tau(t)$ is the logarithm of the dissipation. Kolmogorov's (1962) RSH has been written in the Eulerian frame. The Lagrangian analogy assumes that, in the inertial range, the variance of $X_\tau(t)$ has a logarithmic decrease, i.e.

$$\sigma^2(\tau) = A - \beta\ln(\tau) \tag{2.2}$$

in which σ^2 stands for the variance of X_τ, β is a universal constant and A might depend on the flow (Kolmogorov 1962). A qth-order moment of ϵ_τ is expected to have a power-law behaviour in the inertial range, i.e.

$$M_q(\tau) = \langle \epsilon_\tau^q \rangle \sim \tau^{-K_L(q)}. \tag{2.3}$$

This relation can be completed by a logarithmic decrease of the autocorrelation function of $X(t) = \ln(\epsilon(t))$ associated with multifractal cascades (Arneodo *et al.* 1998), i.e.

$$\rho(\tau) = \langle \tilde{X}(t)\tilde{X}(t+\tau)\rangle = A' - \beta'\ln(\tau) \tag{2.4}$$

in which $\tilde{X} = X - \langle X \rangle$. For a lognormal cascade, we expect $\mu = K_L(2) = \beta = \beta'$, in which μ is the intermittency parameter (Schmitt 2003). On the other hand, one expects also a power-law behaviour for the qth-order LSF, $S_q^L(\tau) \sim \tau^{\zeta(q)}$. The LRSH assumes a relationship between these two quantities, i.e.

$$S_L^q(\tau) \sim \langle \epsilon_\tau^{q/2} \rangle \tau^{q/2} \sim \tau^{q/2 - K_L(q/2)} \tag{2.5}$$

leading to a relation between scaling exponents, i.e.

$$\zeta_L(q) = q/2 - K_L(q/2). \tag{2.6}$$

Let us note that this scaling relation (equation (2.6)) can be found for non-lognormal cascades so that the original Kolmogorov assumption of lognormality is not included in the RSH. The original RSH in the Eulerian frame has been very well verified (Stolovitzky, Kailasnath & Sreenivasan 1992; Stolovitzky & Sreenivasan 1994; Chen *et al.* 1997; Praskovsky, Praskovskaya & Horst 1997). However, only few works have tested the RSH in the Lagrangian frame (Chevillard *et al.* 2003; Benzi *et al.* 2009; Yu & Meneveau 2010; Homann, Schulz & Grauer 2011; Sawford & Yeung 2011). For example, Chevillard *et al.* (2003) proposed a multifractal formula to describe the Lagrangian velocity increments. It is found that the left part of the measured singularity spectrum $D(h)$ agrees well with both the lognormal model and the log-Poisson model. Yu & Meneveau (2010) investigated the Lagrangian time correlation function $\rho(\tau)$ for both Lagrangian strain- and rotation-rate tensors. They found that the correlation function $\rho(\tau)$ depends on the spatial location of particles released. Benzi *et al.* (2009) tested the LRSH along Lagrangian trajectories. They showed that the LRSH is well verified by making extended self-similarity plots. Homann *et al.* (2011) studied a conditional Lagrangian increment statistics. They found that the intermittency is significantly reduced when the LSF is conditioned on the energy dissipation rate or similar quantities (e.g. square of vorticity). A similar result has been shown for the Eulerian velocity structure function: it is found that if one removes strong dissipation events, the corresponding scaling exponent is then approaching the Kolmogorov's (1941) ones without intermittent correction (Kholmyansky & Tsinober 2009). Note that in all of these studies, the relation (2.6) was not tested directly.

We would like to provide a comment on the LSF. It has been shown that due to the influence of large-scale motions, known as the infrared effect, and to the contamination of small scales, known as ultraviolet effect, the classical LSF mixes the large- and small-scale information (Huang *et al.* 2013). Therefore, without the help of extended self-similarity (ESS), the LSF cannot identify the correct scaling behaviour of the Lagrangian velocity (Mordant *et al.* 2002; Xu *et al.* 2006*a*; Sawford & Yeung 2011; Falkovich *et al.* 2012). With the help of a fully adaptive method, namely Hilbert–Huang transform, a clear inertial range can be found (Huang *et al.* 2013). In this paper, the LRSH is verified by considering (2.2)–(2.4) and (2.6), where the scaling exponents for the Lagrangian velocity are extracted by using a Hilbert-based method.

3. Numerical validation

The dataset considered here is composed of Lagrangian velocity trajectories in a homogeneous and isotropic turbulent flow obtained from a 2048^3 direct numerical simulation (DNS) with a Reynolds number $Re_\lambda = 400$. We recall briefly some key parameters of this database. There are $\sim 2 \times 10^5$ fluid tracer trajectories, each composed by $N = 4720$ time samplings saved every $0.1\tau_\eta$ time units, in which τ_η is the Kolmogorov time scale. Hence, we can access time scales in the range $0.1 < \tau/\tau_\eta < 236$. The integral time scale T_L is estimated by using the well-known Kolmogorov scaling relation, i.e. $T_L/\tau_\eta = Re^{1/2} \simeq 155$, in which $Re = 3Re_\lambda^2/20$ (Pope 2000). The full energy dissipation rate $\epsilon(t)$ is retrieved from this database along the Lagrangian trajectories. Previously, an inertial range $0.01 < \omega\tau_\eta < 0.1$ (respectively

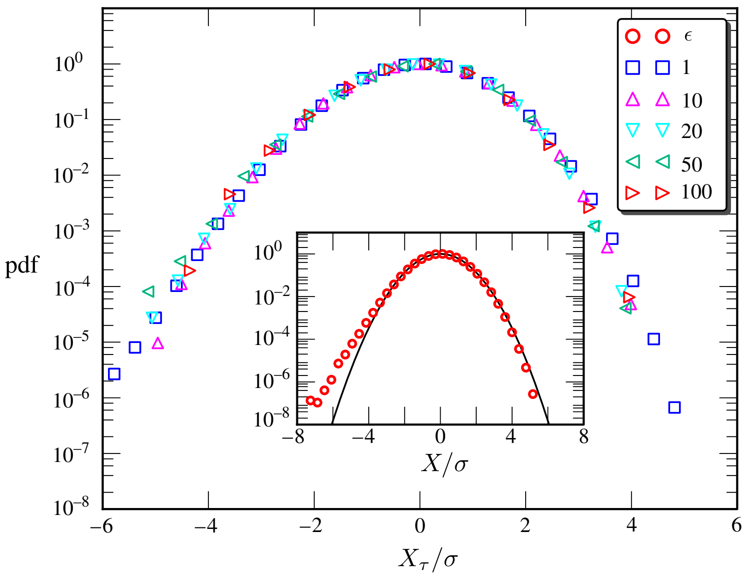

FIGURE 1. Measured p.d.f. of the $X = \ln(\epsilon)$ and local averaged $X_\tau = \ln(\epsilon_\tau)$ for several time scales in both dissipative ($\tau/\tau_\eta < 10$) and inertial ($\tau/\tau_\eta \geqslant 10$) ranges. For comparison, the normal distribution is illustrated by a solid line. Graphically, except for values with $|X_\tau| > 4\sigma$, the measured p.d.f.s agree well with the lognormal distribution. Note that for display clarity, the measured p.d.f. has been centred and vertically shifted by plotting $p(X_\tau) = p_\tau(X_\tau)/p_{max}(\tau)$, in which $p_{max}(\tau) = \max_{X_\tau}\{p_\tau(X_\tau)\}$.

$10 < \tau/\tau_\eta < 100$ or $0.065 < \tau/T_L < 0.65$) has been reported for this database by using a Hilbert-based methodology (Huang *et al.* 2013). We therefore focus on this inertial range in the following analysis. The details of this database can been found in Benzi *et al.* (2009).

Figure 1 shows the measured probability density function (p.d.f.) $p(X)$ and $p_\tau(X_\tau)$ for time scales in the dissipative ($\tau/\tau_\eta < 10$) and inertial ($\tau/\tau_\eta > 10$) ranges. For display clarity, the measured $p_\tau(X_\tau)$ have been centred and vertically shifted by taking $p(X_\tau) = p_\tau(X_\tau)/p_{max}(\tau)$, in which $p_{max}(\tau) = \max_{X_\tau}\{p_\tau(X_\tau)\}$. For comparison, the Gaussian distribution is illustrated as a solid line. Graphically, the measured p.d.f. is slightly deviating from the Gaussian distribution when $|X| > 4\sigma$. This confirms that the lognormal assumption for the energy dissipation rate approximately holds also in the Lagrangian frame at least for the central part of the p.d.f. for $|X| < 4\sigma$.

Figure 2 shows the measured maximum value of the p.d.f. $p_{max}(\tau) - p_{max}(0)$, in which the inertial range $10 < \tau/\tau_\eta < 100$ is indicated by a dashed line. Here $p_{max}(0)$ is for the original energy dissipation rate. A power-law behaviour is observed on the inertial range, i.e.

$$p_{max}(\tau) - p_{max}(0) \sim \tau^{\alpha} \tag{3.1}$$

with a measured scaling exponent $\alpha = 0.81 \pm 0.03$. Note that the statistical error of α is the difference between the scaling exponent fitted on the first and second half of the inertial range (in log scale). In the upper inset, we show the measured $p_{max}(\tau)$, in which the solid line is the power-law fitting. In the lower inset we show the compensated curve $(p_{max}(\tau) - p_{max}(0))\,\tau^{-0.81}$ to emphasize the observed power law.

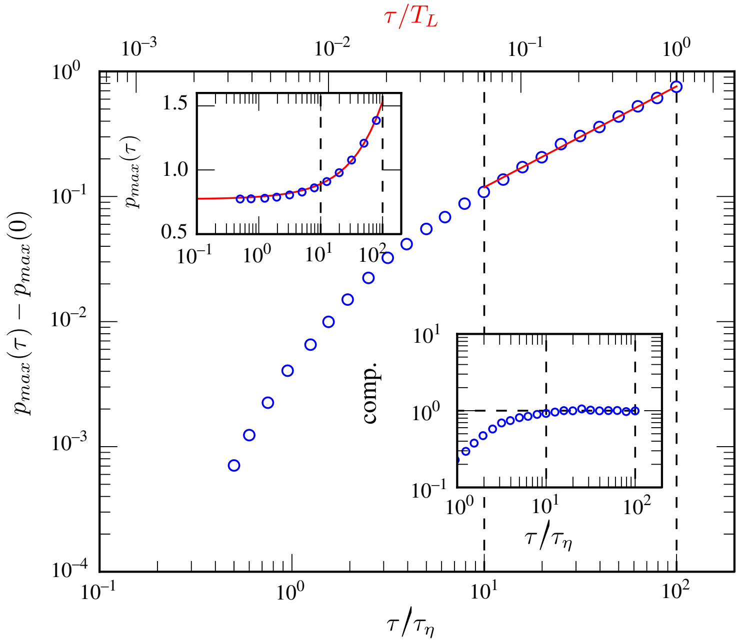

FIGURE 2. Measured max value of p.d.f.s, $p_{max}(\tau) - p_{max}(0)$, in which the inertial range $10 \leqslant \tau/\tau_\eta \leqslant 100$ is illustrated by a dashed line. The upper inset shows the measured $p_{max}(\tau)$, in which the solid line is the power-law fitting. The lower inset shows the compensated curve $(p_{max}(\tau) - p_{max}(0))\ \tau^{-0.81}$. A power-law behaviour is observed in the inertial range $10 < \tau/\tau_\eta < 100$ with a scaling exponent $\alpha = 0.81 \pm 0.03$. The statistical error of α is the difference between the scaling exponent fitted on the first and second half of the scaling range (in log scale).

A plateau is observed in the inertial range. To the best of the authors' knowledge, it is the first time that this p.d.f. scaling relation has been found. We have no interpretation presently for this relation and for the value of its exponent α.

Figure 3 shows the measured Fourier power spectrum of $X = \ln(\epsilon)$. A power-law behaviour is observed in the range $0.01 < f\tau_\eta < 0.06$ with a scaling exponent 1.06 ± 0.13. The inset shows a compensated curve by using the fitted parameters to emphasize the observed power-law behaviour. Figure 4 shows the measured variance $\sigma^2(\tau)$ of $\ln(\epsilon_\tau(t))$ ($\circ$). A log-law is observed for $\sigma^2(\tau)$ respectively on the range $10 < \tau/\tau_\eta < 100$ with a scaling exponent $\beta = 0.30 \pm 0.01$. The inset shows the corresponding compensated curve to emphasize the observed log-law. Equation (2.2) is thus verified. Note that the $1/f$ type Fourier power spectrum is a consequence of a multiplicative cascade. Hence, this result is consistent with the logarithmic decay of the variance observed here. We also note that Pope & Chen (1990) have proposed an Ornstein–Uhlenbeck process for the dissipation field, which would predict a Lorentzian (or Cauchy) spectrum, i.e. a f^{-2} decreasing. Here the observed $1/f$ spectrum does not support the Ornstein–Uhlenbeck proposal.

Figure 5 shows the measured autocorrelation function $\rho(\tau)$ for both the logarithm of the energy dissipation rate ϵ ($\circ$) and pseudo-dissipation $\epsilon_T = \nu(\partial u_i/\partial x_j)(\partial u_i/\partial x_j)$ ($\square$): (*a*) lin–lin plot; (*b*) semilog *x* plot; and (*c*) semilog *y* plot, respectively. The measured $\rho_\epsilon(\tau)$ and $\rho_{\epsilon_T}(\tau)$ cross zero at $\tau/\tau_\eta \simeq 23$. This is consistent with the observation of Pope (1990). We test the log-law, i.e. (2.4) first, see figure 5(*b*). A log-law is observed

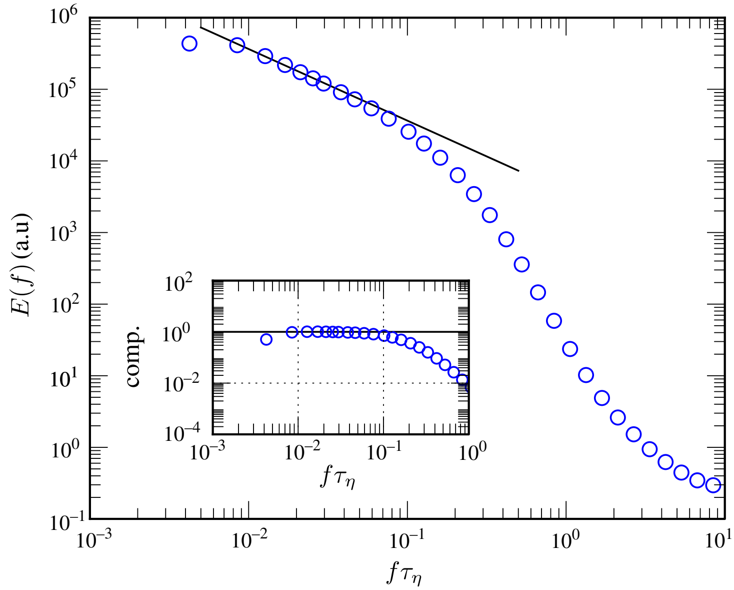

FIGURE 3. Measured Fourier power spectrum of $\ln(\epsilon)$. A power-law behaviour is observed on the range $0.01 < f\tau_\eta < 0.06$ with a scaling exponent 1.06 ± 0.13. The inset shows the compensated curve with fitted parameters.

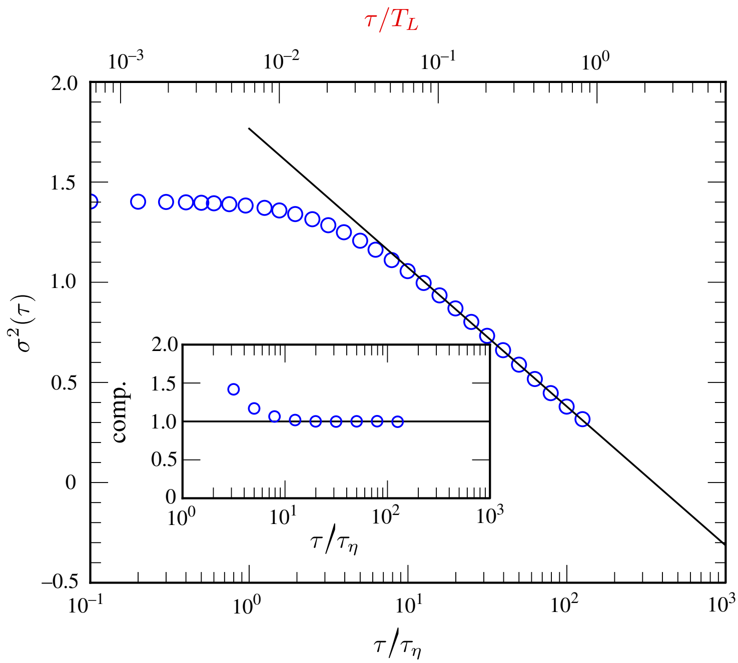

FIGURE 4. Measured variance $\sigma^2(\tau)$ (∘) of $\ln(\epsilon_\tau)$ (∘). A log-law is observed with a scaling exponent $\beta = 0.30 \pm 0.01$ on the range $10 < \tau/\tau_\eta < 100$. The inset shows the compensated curve with fitted parameters to emphasize the log-law. The statistical error of β is estimated as in figure 2.

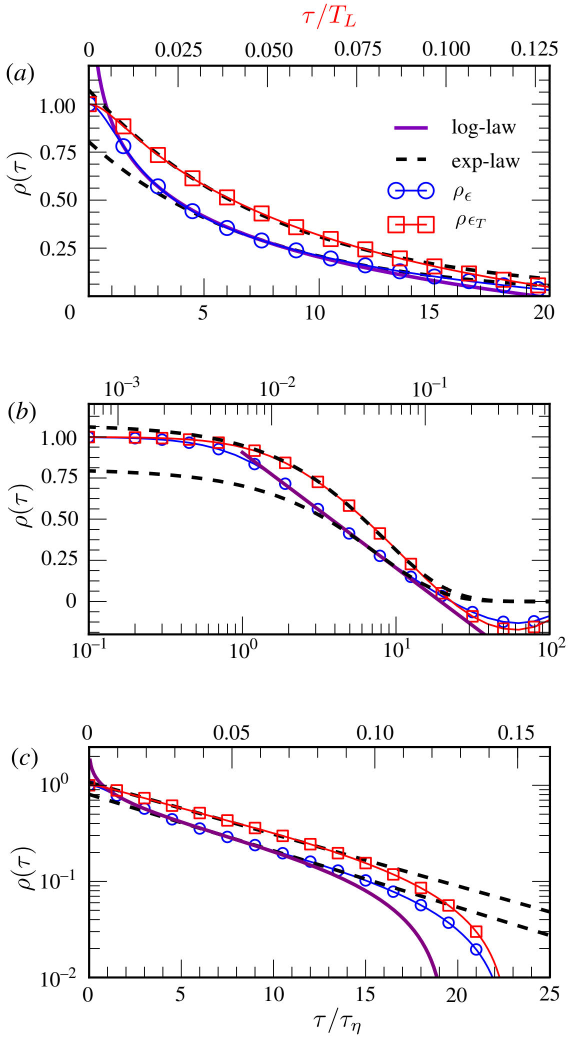

FIGURE 5. Measured autocorrelation function $\rho(\tau)$ for the logarithm of the energy dissipation rate ϵ ($\circ$) and pseudo-dissipation ϵ_T ($\square$): (*a*) lin–lin plot, in which the dashed line and solid line are respectively exponential and logarithmic fitting; (*b*) semilog *x* plot and (*c*) semilog *y* plot. An exponential law is observed on the range $3 < \tau/\tau_\eta < 15$ (respectively $0.019 < \tau/T_L < 0.097$) for ϵ and on the range $0 < \tau/\tau_\eta < 15$ (respectively $0 < \tau/T_L < 0.097$) for ϵ_T. Log-law fitting is observed on the range $1 < \tau/\tau_\eta < 15$ (respectively $0.0065 < \tau/T_L < 0.097$) with a scaling exponent $\beta' = 0.30 \pm 0.01$ for the full dissipation ϵ, verifying (2.4).

for the dissipation ϵ on the range $1 < \tau/\tau_\eta < 15$ ($0.0065 < \tau/T_L < 0.097$) with a scaling exponent $\beta' = 0.30 \pm 0.01$. However, the log-law is less pronounced for the pseudo-dissipation. The log-law is illustrated by a thick solid line in figure 5. We note that Pope & Chen (1990) observed an exponential decay of $\rho(\tau)$. Figure 5(*c*) shows the measured $\rho(\tau)$ in semilog *y* plot. An exponential law is observed respectively on the range $3 < \tau/\tau_\eta < 15$ ($0.019 < \tau/T_L < 0.097$) for ϵ and $0 < \tau/\tau_\eta < 15$ ($0 < \tau/T_L < 0.097$) for ϵ_T. The exponential law is represented by a dashed line in figure 5. Moreover, the

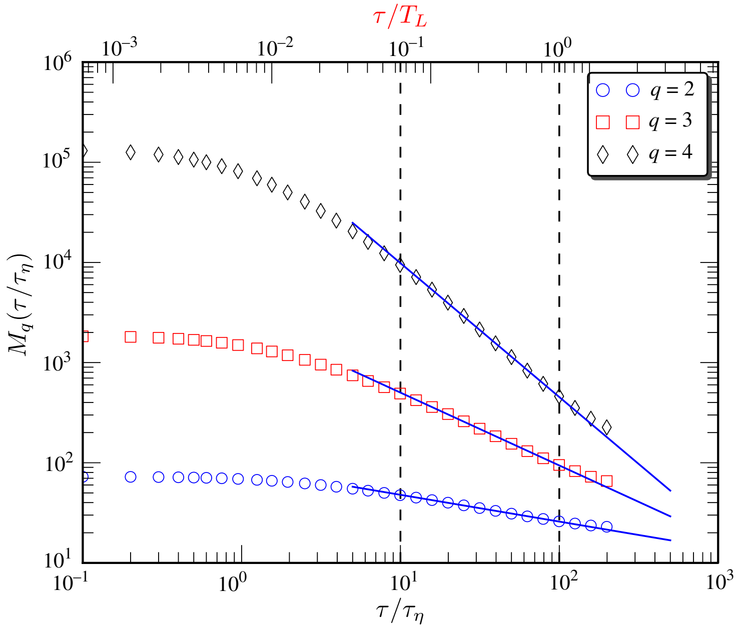

FIGURE 6. Measured $M_q(t/\tau)$ for $q=2$, 3 and 4, in which the inertial range $10\leqslant \tau/\tau_\eta \leqslant 100$ is indicated by a dashed vertical line. Power-law behaviour is observed on this inertial range for all moments we considered here. The scaling exponents $K_L(q)$ are then estimated on this inertial range.

exponential law of pseudo-dissipation is more pronounced than that of full dissipation. Visually, it is difficult to make a distinction between logarithmic and exponential laws. However, we note that an exponential decay as found by Pope & Chen (1990) is not compatible with the intermittency framework for Lagrangian statistics, which is now well accepted (Chevillard *et al.* 2003; Biferale *et al.* 2004). Despite the scaling range, equation (2.4) is verified. Note that the autocorrelation function can be related to the Fourier power spectrum via $\rho(\tau)=\int_0^{+\infty} E(f)\cos(2\pi f\tau)\,\mathrm{d}f$, in which $E(f)$ is the Fourier power spectrum of X. Therefore, except for $f=(n+1/2)/2\tau$, $n=0, 1, 2, \ldots$, all Fourier modes contribute to $\rho(\tau)$, indicating a mixing of large- and small-scale information. This could be one reason for the shift of the scaling range. A similar phenomenon is observed for the structure function, which could be understood as a finite size effect of the range of the power law, known as the infrared effect (large-scale motions) and ultraviolet effect (small-scale motions) (Huang *et al.* 2010, 2013).

The intermittency parameter $\mu = 2 - \zeta_L(4) = 0.30 \pm 0.14$ provided by the Hilbert method (Huang *et al.* 2013) is consistent with the scaling exponents β and β' we obtained here. Let us note here that the covariance log-relation was not a hypothesis of Kolmogorov, and is a relation which is different from (2.2). However there are some relations between them: for a lognormal multiplicative cascade with intermittency parameter $\mu=K_L(2)$, it can be shown that the covariance of X should have a log-law with parameter $\beta'=\mu$ (Kahane 1985). Kolmogorov's hypothesis for the variance of X_τ is also a consequence of the cascade and its parameter is $\beta=\mu$. Here we find $\mu=0.30$ and the values for the slopes of the covariance and variance rescaling, are fully compatible with this value of the intermittency parameter. We also note that the

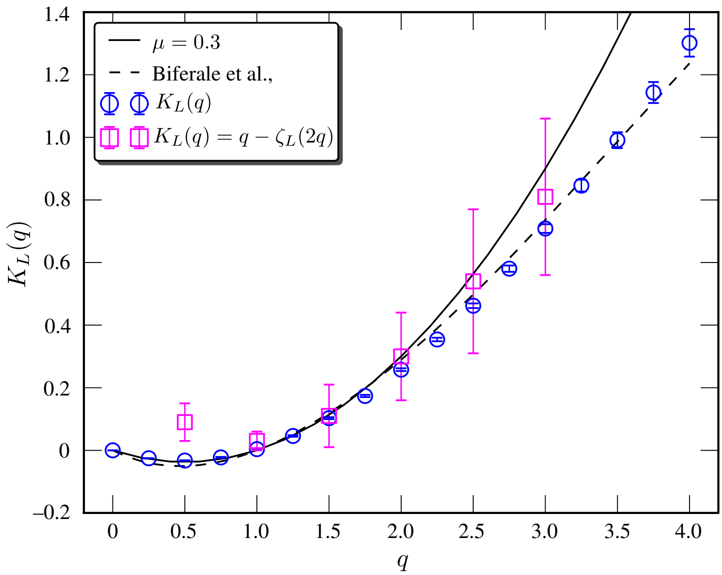

FIGURE 7. Measured $K_L(q)$ (○) and $q - \zeta_L(2q)$ (□) provided by a Hilbert method. For comparison, the curve predicted by the lognormal model with an intermittent parameter $\mu = 0.30$ (solid line) and the log-Poisson-based multifractal model (dashed line) are also shown. The errorbar is the difference between the scaling exponent fitted on the first and second half of the inertial range (in log scale).

direct estimation of the intermittency parameter from the Eulerian structure function is $\mu_E = 2 - \zeta(6) = 0.34 \pm 0.03$ (not shown here). It is also compatible with the value we obtain for Lagrangian fluctuations. Furthermore, when the covariance has a logarithmic decay, the Fourier power spectrum has a -1 scaling, also found here. All of these results are consistent, and confirm that the dissipation in the Lagrangian frame can be described by a multiplicative cascade.

Figure 6 shows the measured $M_q(\tau)$ for $q = 2$, 3 and 4. Power-law behaviour is observed for all moments on the inertial range $10 < \tau/\tau_\eta < 100$. The scaling exponent $K_L(q)$ is then estimated on this range. Figure 7 shows the measured $K_L(q)$ (○) on the range $0 < q < 4$. The errorbar is the difference between the scaling exponent fitted on the first and second half of the inertial range (in log scale). For comparison, $K_L(q) = q - \zeta_L(2q)$ (□) provided by the Hilbert-based methodology is also shown. We estimated $\zeta_L(q)$ up to $q = 6$ by using the Hilbert-based method (Huang *et al.* 2013). The corresponding q for $K_L(q)$ is 3. The definition of the errorbar is the same as that for $K_L(q)$. Values of $K_L(q)$ provided by Biferale *et al.*'s (2004) log-Poisson-based multifractal model and by the lognormal model with the intermittency parameter $\mu = 0.30$ are shown as dashed and solid lines, respectively. For $q \leqslant 3$, all symbols collapse, showing the validity of the scaling relation of (2.6) predicted by the LRSH. For $q > 3$, the measured $K_L(q)$ deviates from the lognormal model since the high-order $M_q(\tau)$ corresponds the statistics of the tail of the p.d.f. and we observed deviations from the Gaussian distribution when $X > 4\sigma$.

4. Conclusion

In summary, the scaling statistics of the energy dissipation along the Lagrangian trajectory is investigated by using fluid tracer particles obtained from a high-resolution DNS with $Re_\lambda = 400$. Both the energy dissipation rate ϵ and the local time-averaged ϵ_τ agree reasonably with the lognormal distribution hypothesis. The measured $p_{max}(\tau) - p_{max}(0)$ (maximum value of a p.d.f.) obeys a power law with a scaling exponent 0.81, a result for which we have no theoretical explanation. Several statistics of the energy dissipation are then examined. It is found that the autocorrelation function $\rho(\tau)$ of $\ln(\epsilon(t))$ and variance σ_τ^2 of $\ln(\epsilon_\tau)$ obey log-laws with scaling exponents compatible with the intermittency parameter $\mu = 0.30$ as expected for multiplicative cascades. These results show that the dissipation along Lagrangian trajectories can be modelled by multiplicative cascades. The qth-order moment of ϵ_τ has a clear power law on the inertial range. The LRSH assumptions (2.2) and (2.3), and scaling relation (2.6) are then verified.

Acknowledgements

This work is sponsored by the National Natural Science Foundation of China (under grant numbers 11072139, 11032007, 11272196, 11202122 and 11332006), 'Pu Jiang' project of Shanghai (grant number 12PJ1403500) and the Shanghai Program for Innovative Research Team in Universities. We acknowledge useful discussions with Nicolas Perpete. We thank Professor F. Toschi for sharing his DNS database, which is freely available from the iCFD database and is available for download at http://cfd.cineca.it.

References

ARNEODO, A., BACRY, E., MANNEVILLE, S. & MUZY, J. F. 1998 Analysis of random cascades using space-scale correlation functions. *Phys. Rev. Lett.* **80** (4), 708–711.

BENZI, R., BIFERALE, L., CALZAVARINI, E., LOHSE, D. & TOSCHI, F. 2009 Velocity-gradient statistics along particle trajectories in turbulent flows: the refined similarity hypothesis in the Lagrangian frame. *Phys. Rev.* E **80** (6), 066318.

BIFERALE, L., BOFFETTA, G., CELANI, A., DEVENISH, B. J., LANOTTE, A. & TOSCHI, F. 2004 Multifractal statistics of Lagrangian velocity and acceleration in turbulence. *Phys. Rev. Lett.* **93** (6), 064502.

BORGAS, M. S. 1993 The multifractal Lagrangian nature of turbulence. *Phil. Trans. R. Soc.* A **342** (1665), 379–411.

CHEN, S. Y., SREENIVASAN, K. R., NELKIN, M & CAO, N. Z. 1997 Refined similarity hypothesis for transverse structure functions in fluid turbulence. *Phys. Rev. Lett.* **79** (12), 2253–2256.

CHEVILLARD, L. & MENEVEAU, C. 2006 Lagrangian dynamics and statistical geometric structure of turbulence. *Phys. Rev. Lett.* **97** (17), 174501.

CHEVILLARD, L., ROUX, S. G., LÉVÊQUE, E., MORDANT, N., PINTON, J.-F. & ARNÉODO, A. 2003 Lagrangian velocity statistics in turbulent flows: effects of dissipation. *Phys. Rev. Lett.* **91** (21), 214502.

FALKOVICH, G., XU, H. T., PUMIR, A., BODENSCHATZ, E., BIFERALE, L., BOFFETTA, G., LANOTTE, A. S. & TOSCHI, F. 2012 On Lagrangian single-particle statistics. *Phys. Fluids* **24** (4), 055102.

FRISCH, U. 1995 *Turbulence: The Legacy of AN Kolmogorov*. Cambridge University Press.

HOMANN, H., SCHULZ, D. L. & GRAUER, R. 2011 Conditional Eulerian and Lagrangian velocity increment statistics of fully developed turbulent flow. *Phys. Fluids* **23**, 055102.

HUANG, Y. X., BIFERALE, L., CALZAVARINI, E., SUN, C. & TOSCHI, F. 2013 Lagrangian single particle turbulent statistics through the Hilbert–Huang transforms. *Phys. Rev.* E **87**, 041003(R).

HUANG, Y. X., SCHMITT, F. G., LU, Z. M., FOUGAIROLLES, P., GAGNE, Y. & LIU, Y. L. 2010 Second-order structure function in fully developed turbulence. *Phys. Rev.* E **82** (2), 026319.

KAHANE, J. P. 1985 Sur le chaos multiplicatif. *Ann. Sci. Math. Que.* **9** (2), 105–150.

KHOLMYANSKY, M. & TSINOBER, A. 2009 On an alternative explanation of anomalous scaling and how well-defined is the concept of inertial range. *Phys. Lett.* A **373** (27), 2364–2367.

KOLMOGOROV, A. N. 1941 Local structure of turbulence in an incompressible fluid at very high Reynolds numbers. *Dokl. Akad. Nauk SSSR* **30**, 301.

KOLMOGOROV, A. N. 1962 A refinement of previous hypotheses concerning the local structure of turbulence in a viscous incompressible fluid at high Reynolds number. *J. Fluid Mech.* **13**, 82–85.

MENEVEAU, C. 2011 Lagrangian dynamics and models of the velocity gradient tensor in turbulent flows. *Annu. Rev. Fluid Mech.* **43**, 219–245.

MORDANT, N., DELOUR, J., LÉVEQUE, E., ARNÉODO, A. & PINTON, J.-F. 2002 Long time correlations in Lagrangian dynamics: a key to intermittency in turbulence. *Phys. Rev. Lett.* **89** (25), 254502.

POPE, S. B. 1990 Lagrangian microscales in turbulence. *Phil. Trans. R. Soc.* A **333** (1631), 309–319.

POPE, S. B. 2000 *Turbulent Flows*. Cambridge University Press.

POPE, S. B. & CHEN, Y. L. 1990 The velocity-dissipation probability density function model for turbulent flows. *Phys. Fluids* **2**, 1437–1449.

PRASKOVSKY, A., PRASKOVSKAYA, E. & HORST, T. 1997 Further experimental support for the Kolmogorov refined similarity hypothesis. *Phys. Fluids* **9** (9), 2465–2467.

SAWFORD, B. L. & YEUNG, P. K. 2011 Kolmogorov similarity scaling for one-particle Lagrangian statistics. *Phys. Fluids* **23**, 091704.

SCHMITT, F. G. 2003 A causal multifractal stochastic equation and its statistical properties. *Eur. Phys. J.* B **34** (1), 85–98.

SREENIVASAN, K. R. & ANTONIA, R. A. 1997 The phenomenology of small-scale turbulence. *Annu. Rev. Fluid Mech.* **29**, 435–472.

STOLOVITZKY, G., KAILASNATH, P. & SREENIVASAN, K. R. 1992 Kolmogorov's refined similarity hypotheses. *Phys. Rev. Lett.* **69** (8), 1178–1181.

STOLOVITZKY, G. & SREENIVASAN, K. R. 1994 Kolmogorov's refined similarity hypotheses for turbulence and general stochastic processes. *Rev. Mod. Phys.* **66** (1), 229–240.

TOSCHI, F. & BODENSCHATZ, E. 2009 Lagrangian properties of particles in turbulence. *Annu. Rev. Fluid Mech.* **41**, 375–404.

TSINOBER, A. 2009 *An Informal Conceptual Introduction to Turbulence*. Springer.

XU, H. T., BOURGOIN, M., OUELLETTE, N. T. & BODENSCHATZ, E. 2006*a* High order Lagrangian velocity statistics in turbulence. *Phys. Rev. Lett.* **96** (2), 024503.

XU, H. T., OUELLETTE, N. T. & BODENSCHATZ, E. 2006*b* Multifractal dimension of Lagrangian turbulence. *Phys. Rev. Lett.* **96** (11), 114503.

YEUNG, P. K. 2002 Lagrangian investigations of turbulence. *Annu. Rev. Fluid Mech.* **34** (1), 115–142.

YU, H. D. & MENEVEAU, C. 2010 Lagrangian refined Kolmogorov similarity hypothesis for gradient time evolution and correlation in turbulent flows. *Phys. Rev. Lett.* **104** (8), 084502.